Supplementary Information

Relationship between East Asian Cold Surges and Synoptic Patterns: A New Coupling Framework

Anupam Kumar [1,2,3]*, Edmond Y.M. Lo [2,4], and Adam D. Switzer [2,5,6]

[1] Interdisciplinary Graduate School, Nanyang Technological University, Singapore
[2] Institute of Catastrophe Risk Management, Nanyang Technological University, Singapore
[3] Solar Energy Research Institute of Singapore, National University of Singapore, Singapore
[4] School of Civil and Environmental Engineering, Nanyang Technological University, Singapore
[5] Asian School of Environment, Nanyang Technological University, Singapore
[6] Earth Observatory of Singapore, Nanyang Technological University, Singapore

***** Correspondence: anupam002@e.ntu.edu.sg; Tel.: (+65) 91239811; Fax: (+65) 6791-0676

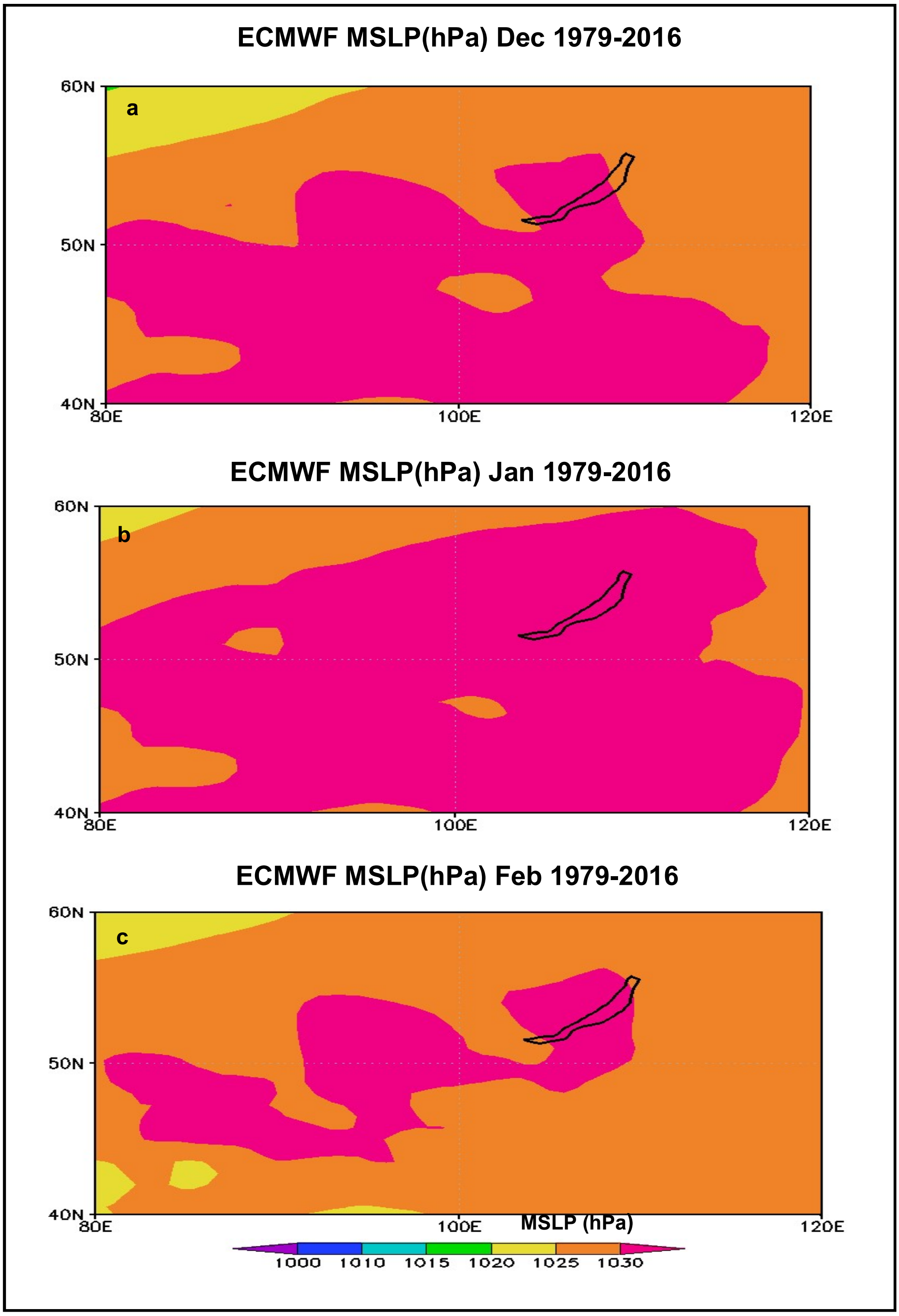

Figure S1. *Differences in SH intensification for (a) December; (b) January; and (c) February during the period 1979-2016. Data from the ECMWF ERA Interim. The coastal boundaries of Lake Baikal are represented by black thick lines.*

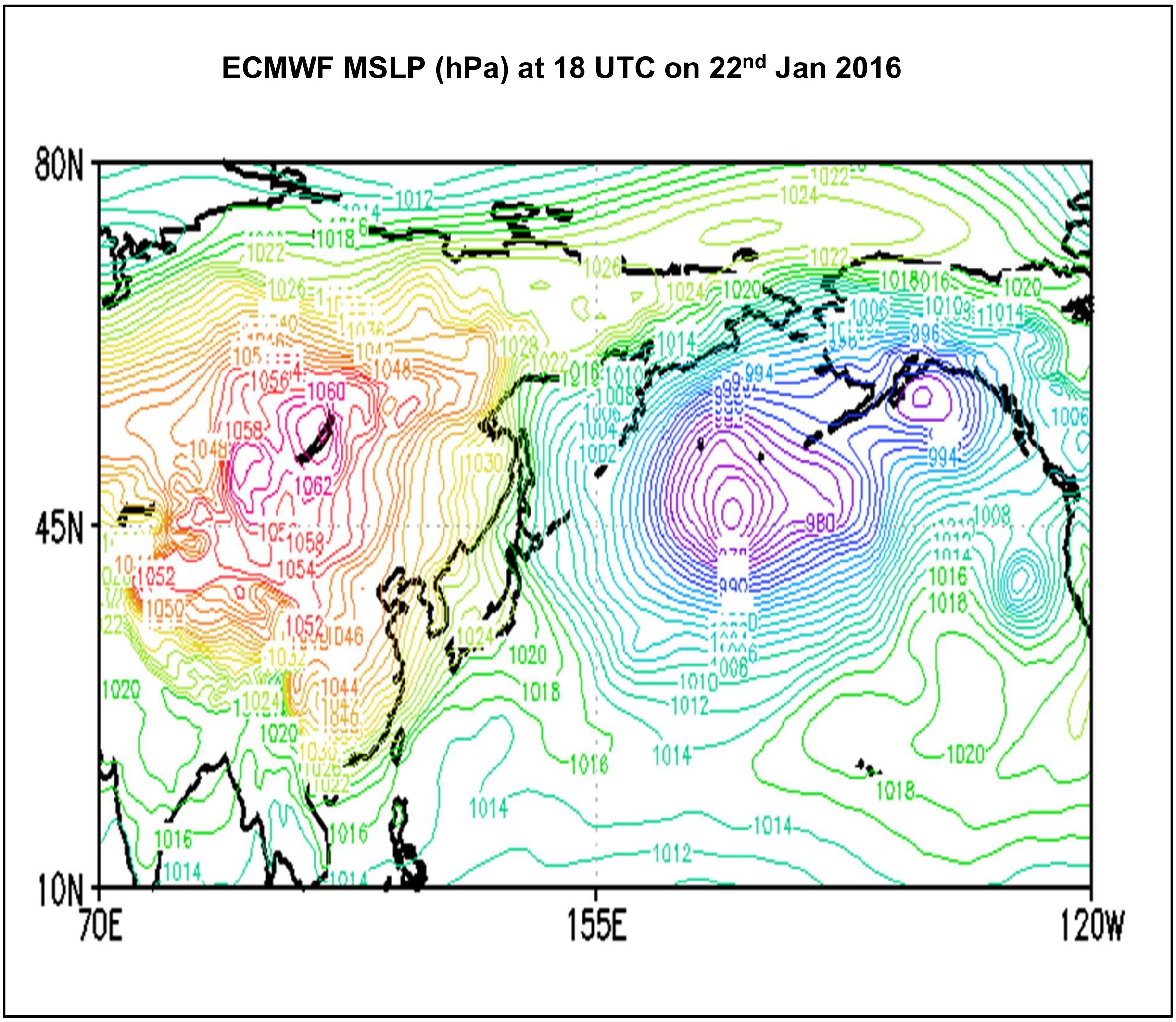

Figure S2. *ECMWF, ERA Interim plots for MSLP at 00 UTC on 22nd Jan 2016 showing formation of intense pressure gradient between SH and AL systems.*

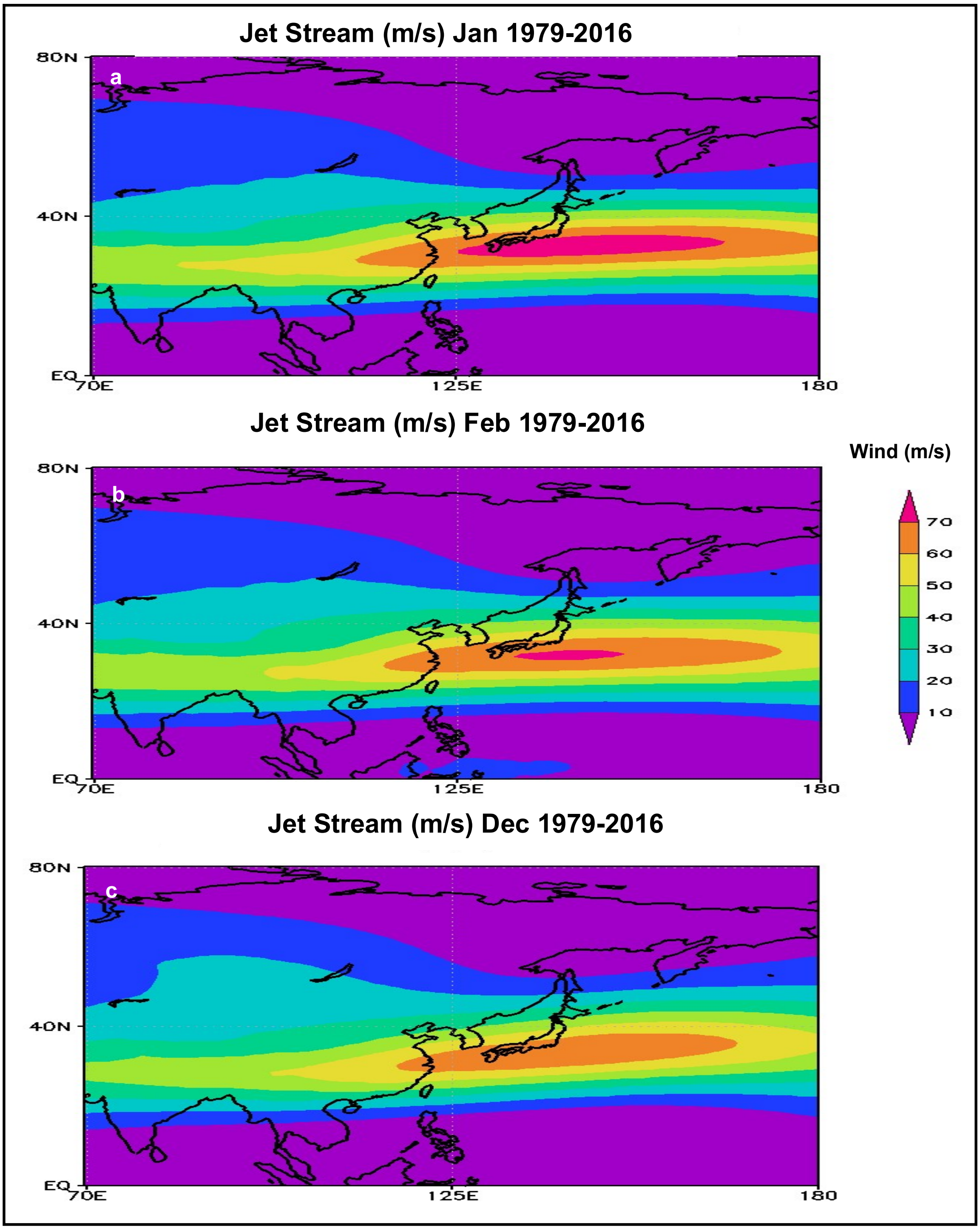

Figure S3. *Differences in JS intensity (m/s) at 250 hPa for (a) December; (b) January; and (c) February during the period 1979-2016. The inner core of JS referred to as Jet Streak (winds above 70 m/s) is evident in Jan and weakens in Feb. Data from the ECMWF ERA Interim. The coastal boundaries are represented by black thick lines.*

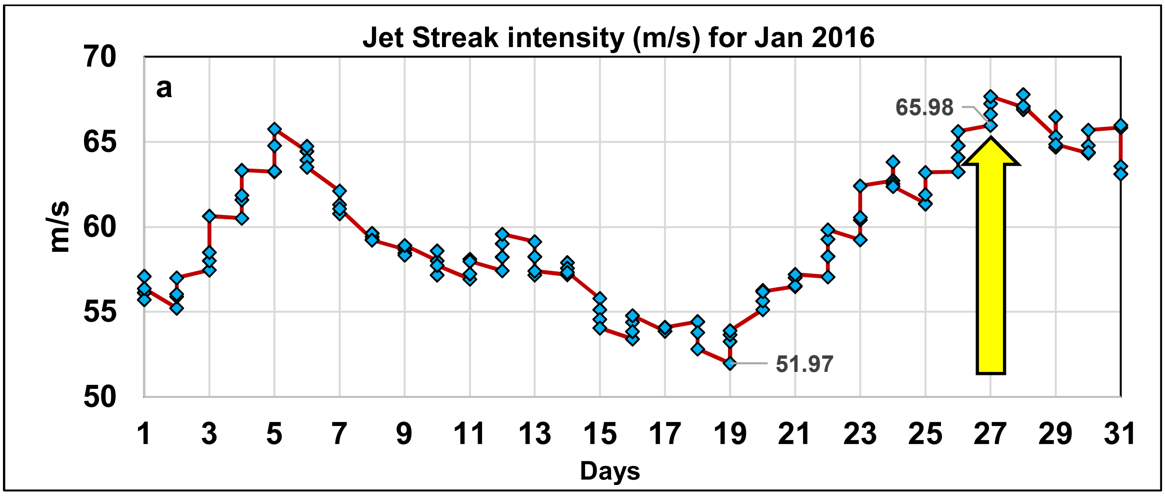

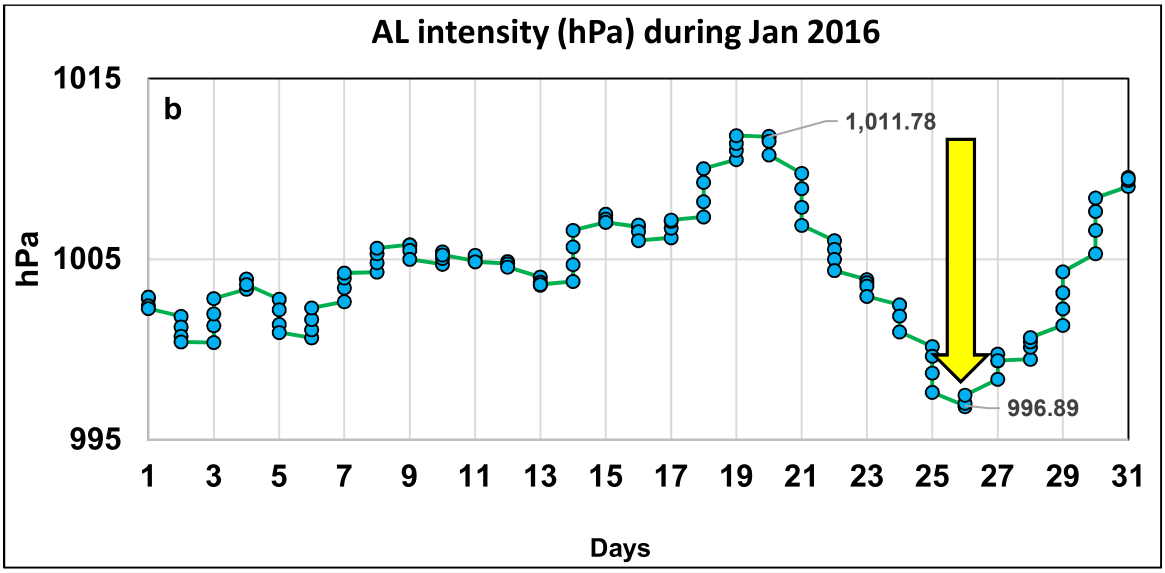

Figure S4. *(a) Jet Streak intensity at 250 hPa (m/s) and (b) AL intensity (hPa) for Jan 2016 at 00, 06, 12, 18 UTC. Yellow arrows in (a) and (b) indicates the maximum intensity of JS and maximum drop in AL attained during the month. Data from the ECMWF, ERA Interim.*

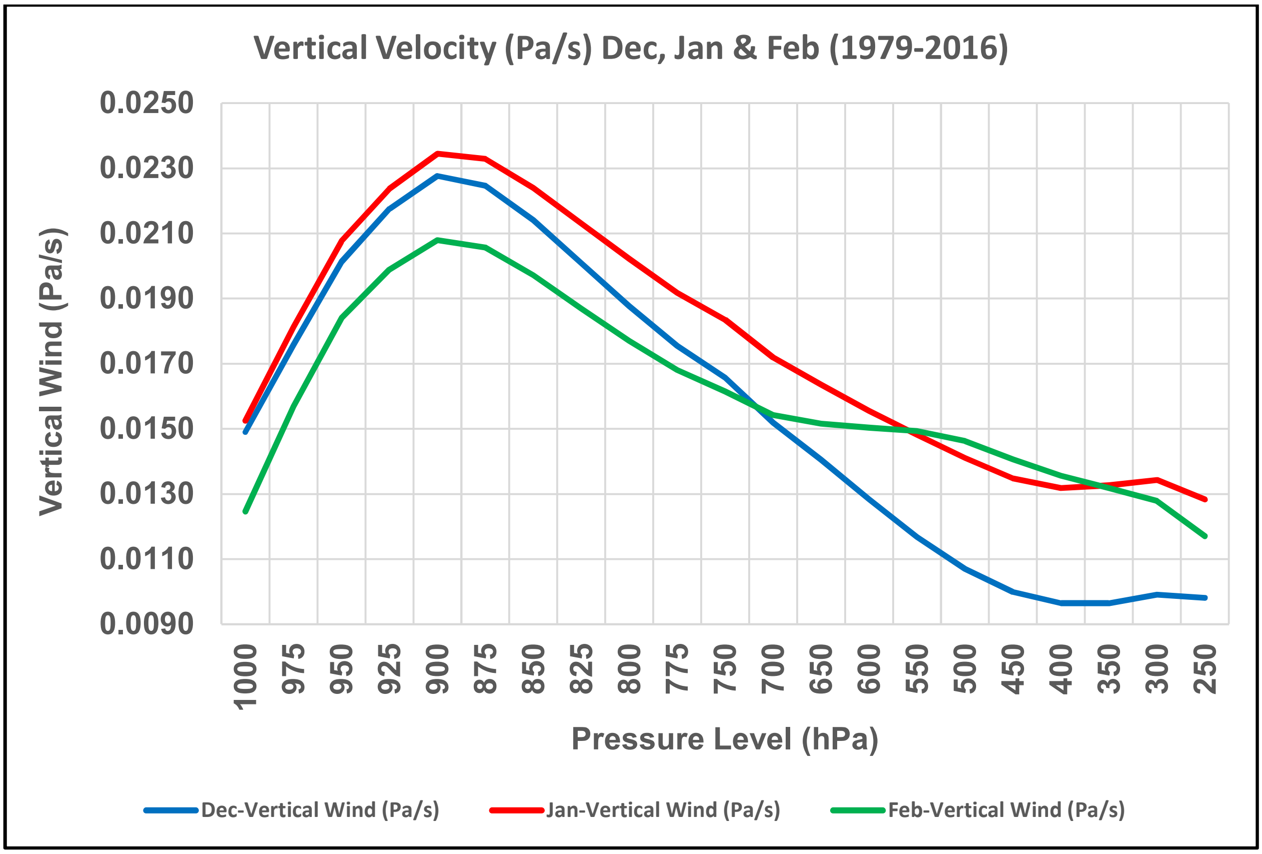

Figure S5. *Vertical velocity (Pa/s) over the active convection region for Dec, Jan and Feb for the period 1979-2016 from 1000 hPa to 250 hPa computed from ECMWF, ERA Interim.*

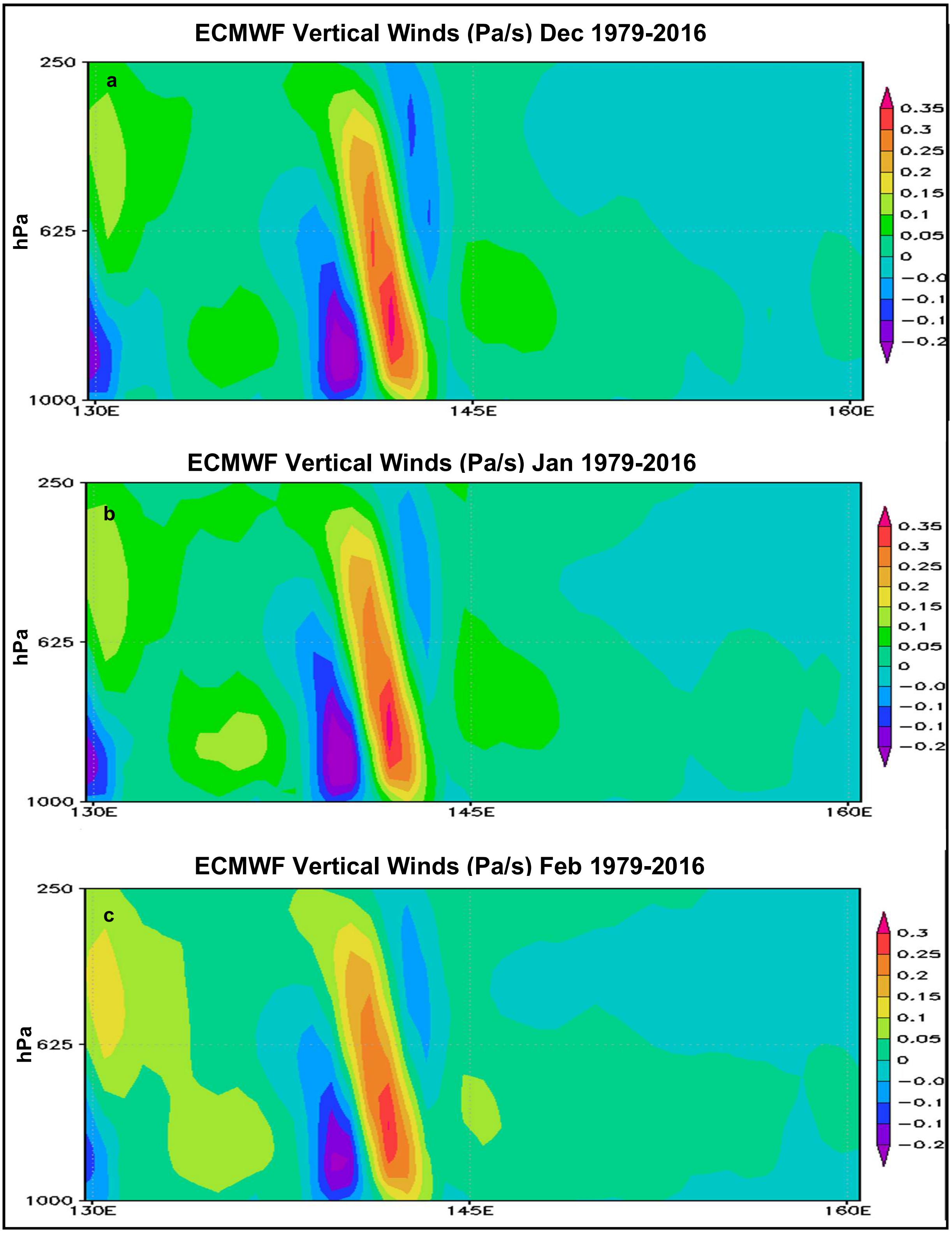

Figure S6. *Vertical winds (Pa/s) at from 1000 hPa to 250 hPa along the cross section at 40 ^{0}N over active convective region for (a) Dec; (b) Jan; and (c) Feb for the period 1979-2016 computed from ECMWF, ERA Interim.*

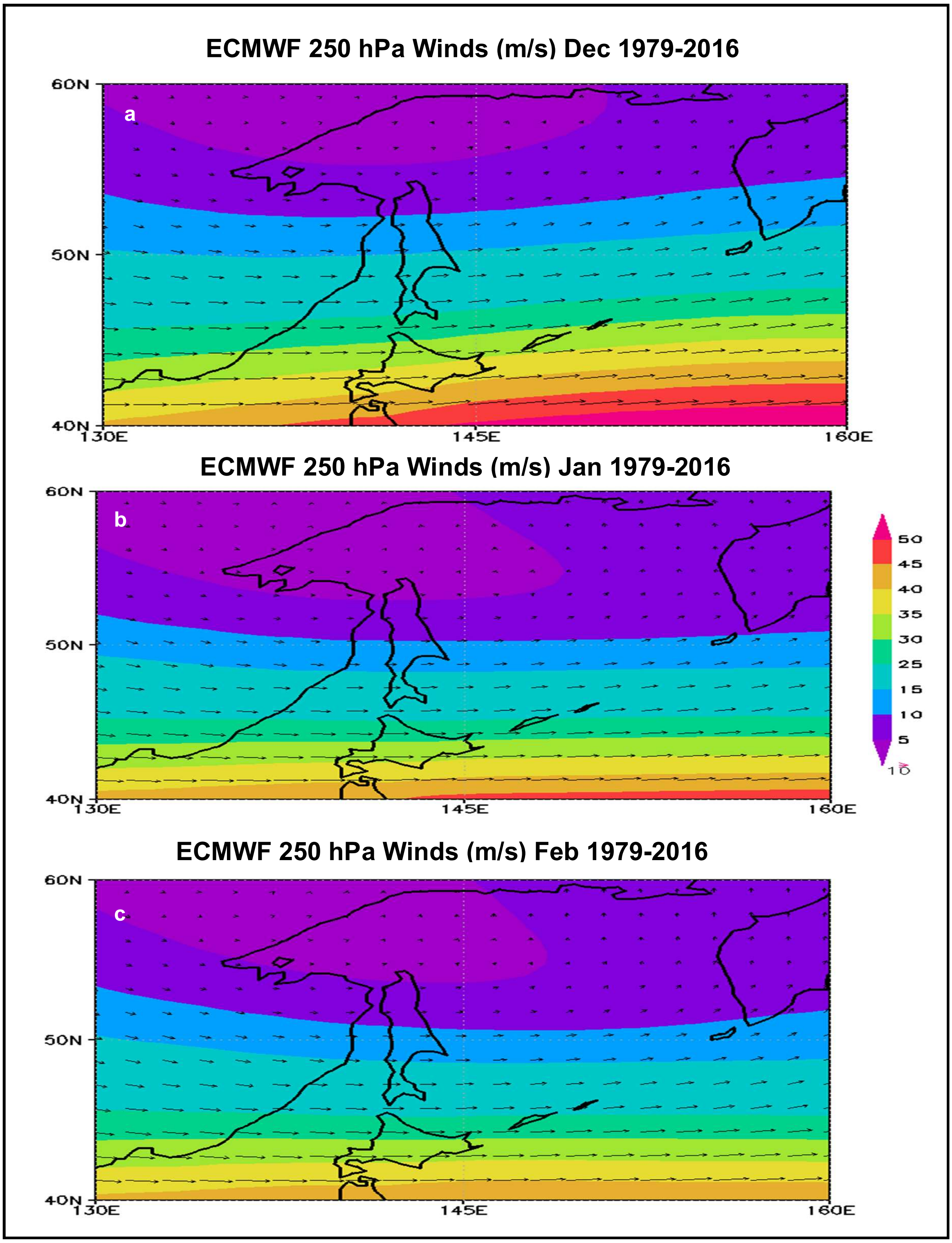

Figure S7. *Climatology of winds (m/s) at 250 hPa over active convective region for (a) Dec; (b) Jan; and (c) Feb for the period 1979-2016 computed from ECMWF, ERA Interim.*

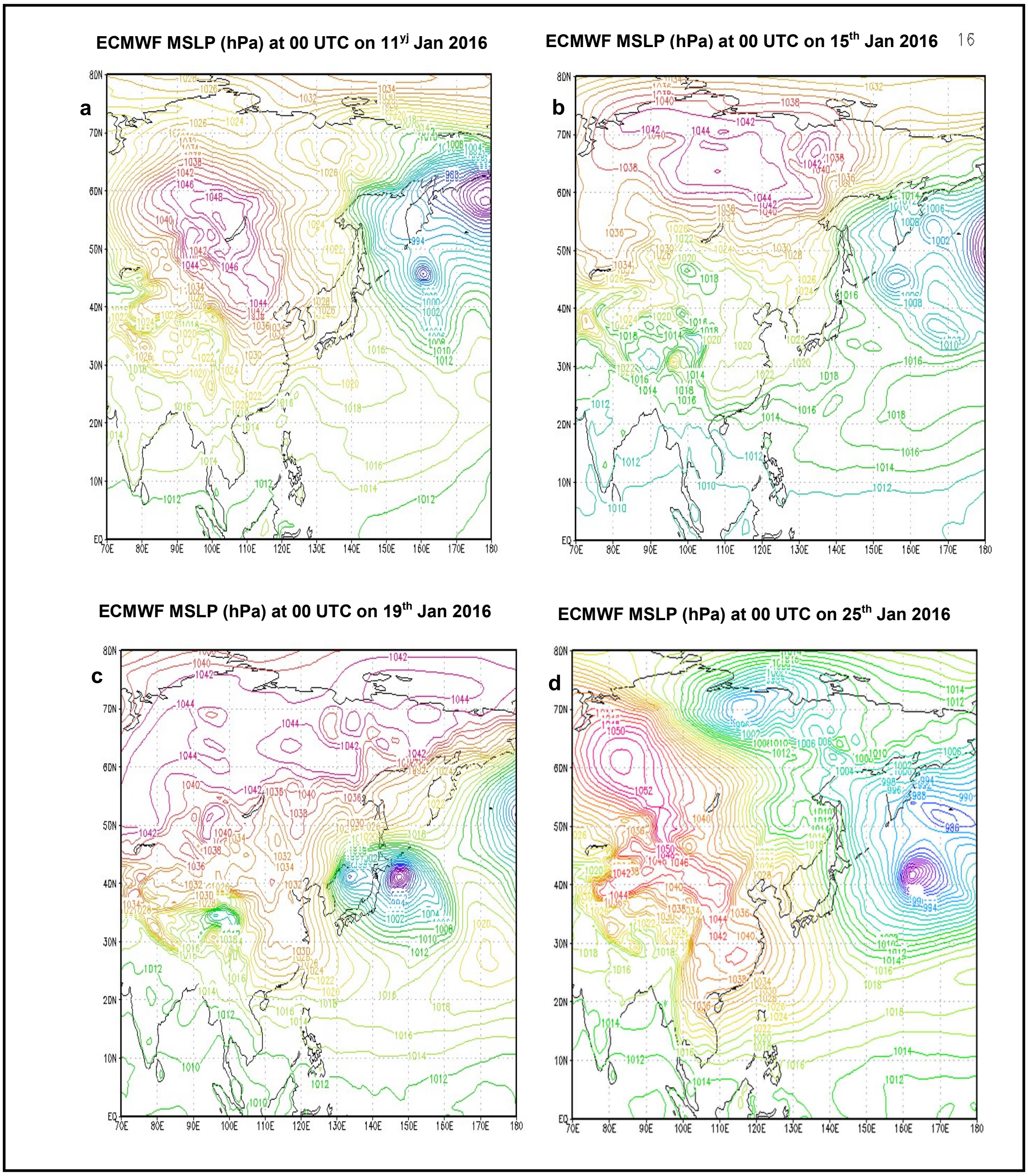

Figure S8. *ECMWF, ERA Interim plots for MSLP at 00 UTC for (a) 11th Jan 2016; (b) 15th Jan 2016; (c) 19th Jan 2016; and (d) 25th Jan 2016 showing formation of frequent LPS during Jan 2016 between 140 ⁰E - 180 ⁰E and 30 ⁰N - 55 ⁰N.*

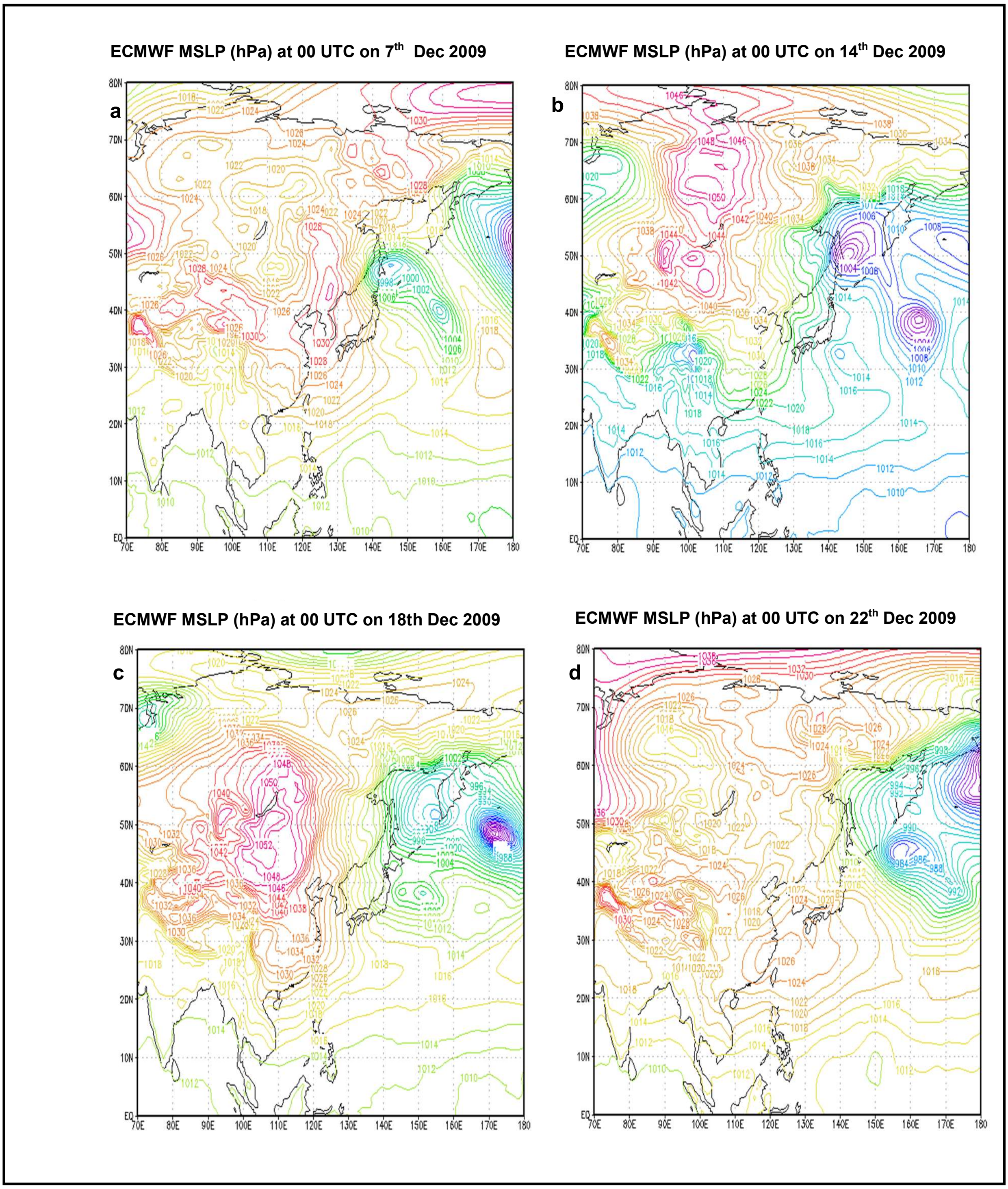

Figure S9. *ECMWF, ERA Interim plot for MSLP at 00 UTC for (a) 7thDec 2009; (b) 14th Dec 2009; (c) 18th Dec 2009; and (d) 22nd Dec 2009 showing formation of frequent LPS during Dec 2009 between 140 ^{0}E - 180 ^{0}E and 30 ^{0}N - 55 ^{0}N.*

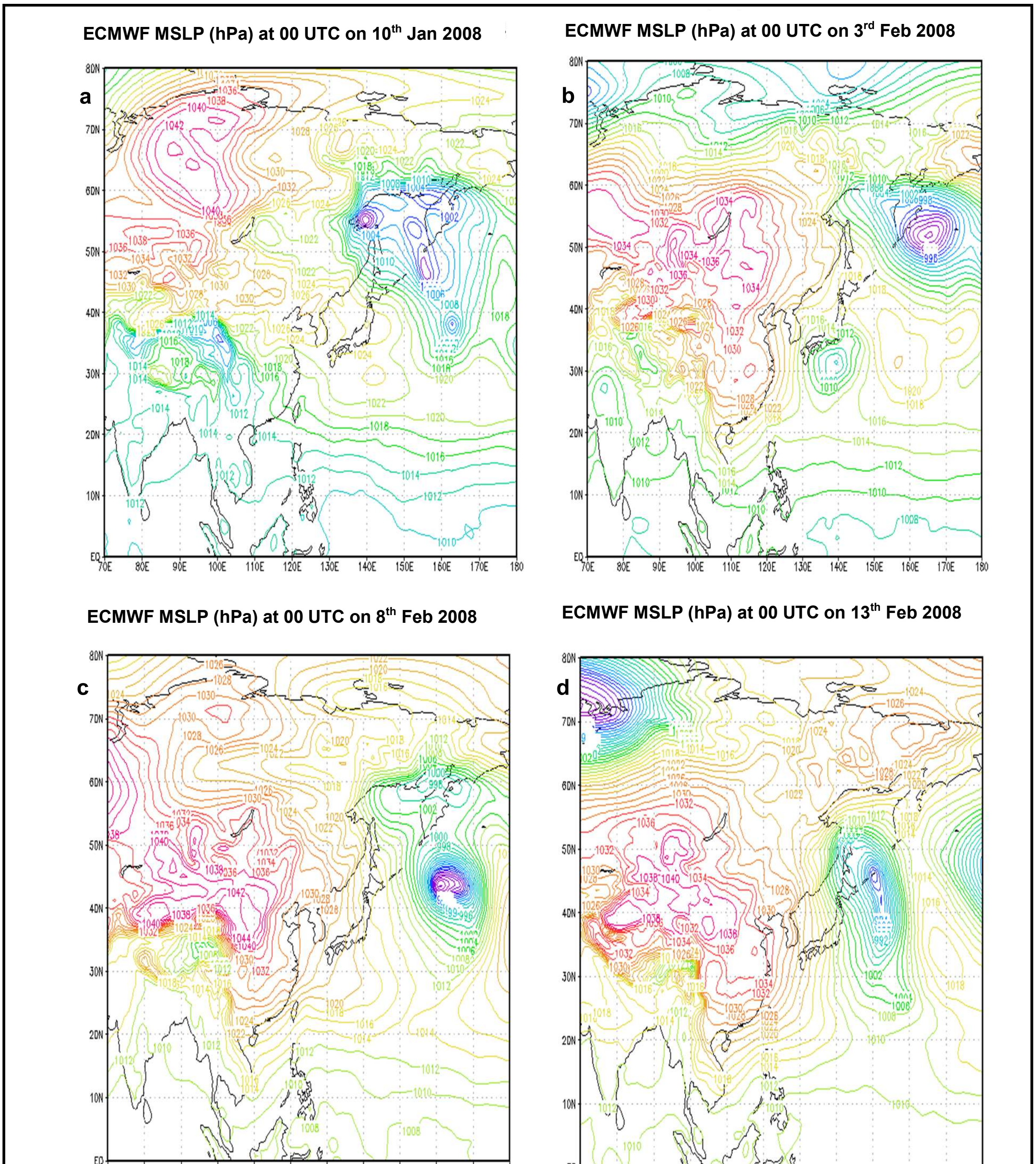

Figure S10. *ECMWF, ERA Interim plot for MSLP at 00 UTC for (a)10th Jan 2008; (b) 3rd Feb 2008; (c) 8th Feb 2008; and (d) 13th Feb 2008 showing formation of frequent LPS during Jan-Feb 2008 between 140 ^{0}E - 180 ^{0}E and 30 ^{0}N - 55 ^{0}N.*

Table S1. Surface temperature anomalies over 2001-2010 with respect to 1961–1990 globally, and in the northern hemisphere and southern hemispheres along with warmest/least warm year during 2001–2010, and warmest/coldest decade over 1881-2010 (adopted from WMO, 2013).

Domain		Temperature Anomaly (^{0}C)		
		2001-2010	Warmest/least warm year during 2001-2010	Warmest/Coldest Decade on record
Global	Land	+0.79 ^{0}C	2007 (+0.95 ^{0}C) 2001 and 2004 (+0.68^{0}C)	2001-2010 (+0.79 ^{0}C) 1881-1890 (-0.51^{0}C)
	Ocean	+0.35 ^{0}C	2003 (+0.40 ^{0}C) 2008 (+0.26^{0}C)	2001-2010 (+0.35 ^{0}C) 1901-1910 (-0.45^{0}C)
	Land-Ocean	+0.47 ^{0}C	2010 (+0.54 ^{0}C) 2008 (+0.35^{0}C)	2001-2010 (+0.47 ^{0}C) 1901-1910 (-0.45^{0}C)
Northern Hemisphere	Land	+0.90 ^{0}C	2007 (+1.13 ^{0}C) 2004 (+0.76^{0}C)	2001-2010 (+0.90 ^{0}C) 1901-1910 (-0.52^{0}C)
	Ocean	+0.41 ^{0}C	2005 (+0.47 ^{0}C) 2008 (+0.33^{0}C)	2001-2010 (+0.41 ^{0}C) 1901-1910 (-0.39^{0}C)
	Land-Ocean	+0.60 ^{0}C	2010 (+0.69 ^{0}C) 2008 (+0.53^{0}C)	2001-2010 (+0.60 ^{0}C) 1901-1910 (-0.38^{0}C)
Southern Hemisphere	Land	+0.48 ^{0}C	2005 (+0.67 ^{0}C) 2001 (+0.34^{0}C)	2001-2010 (+0.48 ^{0}C) 1901-1910 (-0.53^{0}C)
	Ocean	+0.29 ^{0}C	2002 (+0.34 ^{0}C) 2008 (+0.20^{0}C)	2001-2010 (+0.29 ^{0}C) 1901-1910 (-0.51^{0}C)
	Land-Ocean	+0.33 ^{0}C	2009 (+0.38 ^{0}C) 2008 (+0.24^{0}C)	2001-2010 (+0.33 ^{0}C) 1901-1910 (-0.51^{0}C)

Table S2. The World's warmest year on record (adopted from WMO, 2017).

Year	Anomaly with respect to 1981-2010 average (^0C)
2016	+.56
2017	+.46
2015	+.45
2014	+.30
2010	+.28
2005	+.27
2013	+.24
2006	+.22
2009	+.21
1998	+.21